Original Article

Semi-quantitative analysis of pre-treatment morphological and intratumoral characteristics using ^{18}F-fluorodeoxyglucose positron-emission tomography as predictors of treatment outcome in nasal and paranasal squamous cell carcinoma

Noriyuki Fujima[1], Kenji Hirata[2], Tohru Shiga[2], Koichi Yasuda[3,4], Rikiya Onimaru[3], Kazuhiko Tsuchiya[5], Satoshi Kano[6], Takatsugu Mizumachi[6], Akihiro Homma[6], Kohsuke Kudo[1], Hiroki Shirato[3,4]

[1]Department of Diagnostic and Interventional Radiology, Hokkaido University Hospital, Sapporo, Japan; [2]Department of Nuclear Medicine, [3]Department of Radiation Medicine, Hokkaido University Graduate School of Medicine, Sapporo, Japan; [4]The Global Station for Quantum Medical Science and Engineering, Global Institution for Collaborative Research and Education, Sapporo, Japan; [5]Department of Radiation Oncology, Otaru General Hospital, Otaru, Japan; [6]Department of Otolaryngology-Head and Neck Surgery, Hokkaido University Graduate School of Medicine, Sapporo, Japan

Correspondence to: Noriyuki Fujima, MD, PhD. Department of Diagnostic and Interventional Radiology, Hokkaido University Hospital, N15, W7, Kita-Ku, Sapporo 060-8638, Japan. Email: Noriyuki.Fujima@mb9.seikyou.ne.jp.

Background: To investigate the utility of quantitative morphological and intratumoral characteristics obtained by ^{18}F-fluorodeoxyglucose positron-emission tomography/computed tomography (FDG-PET/CT) for the prediction of treatment outcome in patients with nasal or paranasal cavity squamous cell carcinoma (SCC).

Methods: Twenty-four patients with nasal or paranasal cavity SCC who received curative non-surgical therapy (a combination of super-selective arterial cisplatin infusion and radiotherapy) were retrospectively analyzed. From pre-treatment FDG-PET data, a total of 13 parameters of quantitative morphological characteristics (tumor volume, surface area and sphericity), intratumoral characteristics (the maximum and mean standard uptake value, three intratumoral histogram and four textural parameters) and total lesion glycolysis (TLG) were respectively calculated. Information regarding the treatment outcome was determined from the histological diagnosis or clinical follow-up. Each of the 13 quantitative parameters as well as T- and N-stage was assessed for its relation to treatment outcome of local control or failure.

Results: In univariate analysis, significant differences in surface area and sphericity between the local control and failure groups were observed. The receiver operating characteristic (ROC) curve analysis showed that sphericity had the highest accuracy of 0.88. In the multivariate analysis, sphericity was revealed as an independent predictor of the local control or failure.

Conclusions: The quantitative parameters of sphericity are useful to predict the treatment outcome in patients with nasal or paranasal SCC.

Keywords: Head and neck neoplasms; carcinoma, squamous cell; positron-emission tomography

Submitted Jul 03, 2018. Accepted for publication Sep 12, 2018.
doi: 10.21037/qims.2018.09.09
View this article at: http://dx.doi.org/10.21037/qims.2018.09.09

Introduction

Non-surgical treatments such as chemoradiation therapy have been important treatment methods for patients with head and neck squamous cell carcinoma (HNSCC) (1), particularly since they result in less functional impairment than surgical treatment (2). In particular, the combination therapy of super-selective arterial infusions of cisplatin and radiotherapy has become popular because it can achieve a high local control rate even in advanced stage patients with nasal- or paranasal-cavity SCC (3,4). For such a curative nonsurgical treatment, it can be helpful to predict the treatment outcome in order to optimize the subsequent patient management, including the determination of treatment re-planning and the follow-up strategy.

For the evaluation of primary lesions, ^{18}F-fluorodeoxyglucose positron-emission tomography/computed tomography (FDG-PET/CT), which depicts the tumor metabolic rate of glucose, has been a major diagnostic modality. The tumor glucose metabolic rate is one of the important factors reflecting tumor aggressiveness (5,6). Several studies have also investigated FDG-PET/CT parameters, particularly the maximum standardized uptake value (SUVmax), metabolic tumor volume (MTV) and total lesion glycolysis (TLG), for their potential roles in predicting treatment outcomes in HNSCC patients (7-9). Another proposed approach to the evaluation of FDG uptake in HNSCC is determination of the textural features of FDG distribution in the tumor; this method can reveal tumor heterogeneity in greater detail (10-12). In addition, tumor morphological information can also be a useful parameter. FDG-PET/CT data provide rough anatomical information about the tumor revealed by the lesion's elevated FDG uptake. Moreover, the tumor margin can be easily set using the threshold of FDG uptake from FDG-PET/CT imaging, allowing objective quantification of the whole tumor area (13). From this morphological data, several parameters related to the tumor morphological shape can be calculated. FDG-PET/CT analysis can provide many parameters related to morphology or intratumoral characteristics as mentioned above and are also considered to provide useful information for the prediction of treatment outcome as one of imaging biomarker. Some of these parameters may predict the treatment outcome with high diagnostic accuracy.

The aim of this study was to investigate the utility of various semi-quantitative FDG uptake parameters as prognostic factors for patients with nasal- or paranasal-cavity SCC receiving curative super-selective arterial infusion with concomitant radiotherapy.

Methods

Study subjects

Our institutional review board approved this retrospective study protocol, and written informed consent was waived. Twenty-four patients with nasal or paranasal cavity SCC who were treated at our hospital from April 2009 to August 2012 were evaluated. All patients fulfilled the following inclusion criteria: (I) histopathological diagnosis of nasal or paranasal SCC; (II) completion of curative radiotherapy with 70-Gy radiation dose; and (III) availability of pre-treatment FDG-PET/CT data with the specific scan units. All patients were treated using the following protocol: arterial cisplatin infusion (100–120 mg/m^2 per week for 4 weeks) by microcatheter in the feeding arteries of the primary tumor, with concurrent radiation therapy (total 70 Gy/35 fractions). All patients received FDG/PET-CT scans before the full course of treatment.

Clinical assessment

For determination of the final clinical assessment (local control or local failure at the primary lesion), the medical records of patients over the follow-up period were utilized. Local failure was determined by (I) presence of SCC diagnosed by histopathological analysis of surgically resected or biopsy samples, (II) new soft tissue mass development around the post-treatment granulation tissue, or (III) definite enlargement of granulation tissue area during the follow-up. Local control was determined by histopathological diagnosis of the complete absence of SCC in resected tissue, the absence of new lesion development or the enlargement of soft-tissue mass in the post-treatment granulation tissue, during a follow-up of ≥2 years.

Imaging protocol

Image acquisition was performed using a PET/CT scanner (Biograph 64, Asahi-Siemens Medical Technologies, Tokyo). The patients were instructed to fast for ≥6 h before the FDG (4.5 MBq/kg) injection. After the injection, the patients were asked to sit quietly for 60 min. The 425–650 keV of energy window, 58.5 and 21.6 cm of the transaxial and axial fields of view (FOVs) were respectively used for scanning. The 3D-mode emission scan was acquired over 3-min for each bed position. The attenuation correction was performed with X-CT images that were obtained without contrast agent. An iterative technique integrated

with a point spread function (i.e., TrueX) was used for the image reconstruction (14). We conducted the full 3D PET reconstruction with a system matrix derived from point-source measurements. The details of the reconstructed image resolution were as follows: spatial resolution, 8.4 mm full width at half maximum (FWHM); matrix size, 168×168; voxel size, 4.1 mm × 4.1 mm × 2.0 mm. The SUV was calculated as the tissue radioactivity concentration (kBq/mL) divided by the injected dose per body weight (kBq/g) according to the commonly used definition (15).

Image analysis

For the semi-quantitative evaluation of the FDG uptake in the primary tumor, we examined both morphological and intratumoral-characteristic data. Image analyses were performed by a board certified radiologist (Noriyuki Fujima) with 11 years of experience in head and neck radiology. In each tumor, we measured the SUV value with the delineation of the tumor region of interest (ROI). As the tumor ROI, we used the automated ROI determined using the isocontour threshold method. We used an SUV value of 2.5 to define the lesion contouring margins as described in a previous report (16). In addition, another ROI delineation threshold that was adopted in a previous study (=42% of the maximum SUV in the tumor) (17) was also used to validate the measured quantitative parameter values (see the description of the statistical analysis below). When the tumor extended to two or more slices, all slices showing tumor FDG uptake were analyzed. In all patients, both routine CT and magnetic resonance imaging (MRI) data were also used as supplemental information to determine the presence and location of each tumor on FDG-PET/CT images.

For the morphological characteristics analysis, we calculated the tumor volume and tumor surface area from the morphological shape of all selected tumor voxels with an SUV value above 2.5. Sphericity was calculated by a partial modification of the previously reported equations as follows (18,19):

$$Sphericity = \frac{TV}{(1/6)*\sqrt{\frac{TSA^3}{\pi}}}$$

where TV is the tumor volume and TSA is the tumor surface area. The sphericity was defined as the actually measured tumor volume (TV) divided by the calculated volume of the sphere whose surface area was TSA.

For the analysis of intratumoral characteristics, the SUVmean, SUVmax, histogram and textural parameters within the ROI were calculated. SUVmean and SUVmax were respectively calculated as the mean and maximum values in all pixels in all slices in which the tumor was included. The histogram features included the coefficient of variance (CV), kurtosis and skewness. Textural features included the contrast, correlation, energy and homogeneity, calculated based on the gray-level co-occurrence matrix (GLCM) features. The GLCM features comprise detailed information regarding the spatial distribution of signal intensity in the tumor ROI, compared to the histogram parameters. The GLCM is composed of a square plane with rows and columns from zero to the maximum value of the gray scale in the tumor ROI. The GLCM element in row *i* and column *j* represents the number of times a given gray tone of value *i* is horizontally adjacent to gray tone *j* in the original quantized image. For the sake of simplicity the GLCMs were calculated using only directly adjacent pixels. Details of the GLCM features and the calculation equations have been described previously (20). Histogram or texture parameters were calculated from all pixels in all tumor-containing slices; all pixel data were integrated into a single histogram profile or single GLCM feature map to evaluate the whole volume intratumoral characteristics. In addition, TLG was also calculated by multiplying the tumor volume and mean SUV value. Finally, all parameters of morphological features, SUVmax, SUVmean, histogram parameters, textural parameters, and TLG were calculated for each tumor. The calculation process was performed using a self-developed program written in MATLAB ver. 2012a (MathWorks, Natick, MA).

Statistical analysis

In the univariate analysis, we used the Mann-Whitney U-test to compare the values of a total of 13 parameters (SUVmean, SUVmax, CV, TLG, kurtosis, skewness, contrast, correlation, energy, homogeneity, tumor volume, surface area and sphericity) between the local control and failure groups in their primary site. If a significant difference was obtained for any parameter, such parameter was analyzed by receiver operating characteristic (ROC) curves for the calculation of the area under the curve (AUC). The sensitivity, specificity, positive predictive value, negative predictive value and diagnostic accuracy by the cut-off value obtained with the Youden index were respectively determined. If a significant difference was observed for more

Table 1 Patient characteristics

Characteristics	Number of patients
Age (years)	
Range	43–72
Median	61
Average	60.1
Gender	
Male	21
Female	3
T-stage	
T1	0
T2	1
T3	8
T4a	14
T4b	1
N-stage	
N0	21
N1	2
N2	1
N3	0
Clinical TNM-stage	
I	0
II	1
III	8
IV	15

than two parameters in univariate analysis, these parameters were further analyzed by multivariate logistic regression models to determine whether they had independent predictive value. Additionally, if at least one parameter was determined to be an independent predictor, this parameter was further analyzed for its correlation to T-stage, N-stage and other quantitative FDG-PET/CT parameters assessed in the current study, by using Spearman's rank correlation coefficient.

For the validation of parameter value and its diagnostic power, each independent predictor revealed by multivariate logistic regression analysis was re-calculated using a different ROI delineation method with a threshold that was 42% of maximum SUV as described above. The Intraclass Correlation Coefficient (ICC) of parameter values obtained by ROIs between the SUV threshold of 2.5 and 42% of maximum SUV was calculated. The Mann-Whitney U-test and ROC curve analysis were also respectively performed to assess the local control and failure groups in a manner similar to that described above, by using the parameter values obtained by ROIs with an SUV threshold of 42% in maximum SUV.

Statistical significance was set at P values <0.05. We used SPSS software (IBM, Armonk, NY) for the statistical analyses.

Results

The patient characteristics are summarized in *Table 1*. Among the 24 patients, 7 were revealed to have local failure. The local failure of 5 patients was confirmed by histopathological findings. The remaining 2 cases of local failure and 17 cases of local control were confirmed by clinical diagnosis with reference to our hospital medical records over the follow-up period (mean 70 months; range 49–82 months).

All parameters were successfully obtained for each primary site. For two of the parameters, surface area and sphericity, significant differences between the local control and failure groups were respectively revealed in univariate analysis. Details of all obtained parameters and univariate analyses are presented in *Table 2*. These two parameters of the surface area and sphericity were further assessed by ROC curve analysis. Diagnostic values (the AUC, sensitivity, specificity, positive predictive value, negative predictive value, accuracy and cut-off value) for the prediction of the treatment outcome were determined. The details of the ROC curve analysis are presented in *Table 3*. The parameter with the highest AUCs was the sphericity.

In the multivariate analyses, the sphericity was revealed to be an independent predictor (P=0.03) with an odds ratio of 2.58 (the 95% confidence intervals ranged from 1.37 to 6.74) (*Table 3*). Representative cases of local control and failure are presented in *Figure 1*. The Spearman's rank correlation coefficients between the sphericity and patient characteristics (T-stage and N-stage) or other 12 quantitative parameters are summarized in *Table 4*.

In the validation analysis using a different tumor ROI technique, the sphericity was found to be significantly different between patients with local control and failure by the Mann-Whitney U-test (P=0.005). The results of ROC curve analysis were as follows: AUC =0.87, sensitivity =0.82, specificity =1.0, positive predictive value =1.0, negative

Table 2 Patient characteristics and parameters of the patients with local control and failure

Variables	Presence of local control		P value
	Local control	Local failure	
Patients' characteristics (no. of patients)			
T-stage			0.08
T1	0	0	
T2	1	0	
T3	7	1	
T4	9	6	
N-stage			0.86
N0	15	6	
N1	1	1	
N2	1	0	
N3	0	0	
Image parameters (parameter value)			
SUVmean	7.6±2.2	7.5±1.3	0.99
SUVmax	19.3±6.1	18.3±3.6	0.63
CV	0.43±0.11	0.38±0.11	0.34
TLG	274.5±184.3	326.1±112.9	0.39
Skewness	0.85±0.75	0.84±0.52	0.96
Kurtosis	3.7±3.57	3.83±2.75	0.92
Contrast	6.64±2.78	6.85±2.69	0.86
Correlation	0.63±0.11	0.63±0.06	0.8
Energy	0.023±0.011	0.027±0.018	0.68
Homogeneity	0.45±0.06	0.46±0.05	0.72
Tumor volume	33.2±16.7	42.5±9.4	0.09
Tumor surface area	97.8±29.8	143.3±36.5	0.01*
Sphericity	0.35±0.06	0.27±0.05	0.002*

Data are the mean ± standard deviation. *, statistically significant difference. SUV, standardized uptake value; CV, coefficient of variance; TLG, total lesion glycolysis.

predictive value =0.7, accuracy =0.88 and optimal cut-off value =0.35. Only cut-off value was slightly different from the result obtained by the tumor ROI with SUV threshold 2.5. The ICC of the sphericity values obtained by ROIs between the SUV threshold of 2.5 and 42% of maximum SUV was 0.93.

Discussion

In the current study, the semi-quantitative morphological parameter of sphericity was revealed to be a clinically useful predictor of treatment outcome in patients with nasal- or paranasal-cavity SCC. The difficulty of using pretreatment parameters to predict treatment outcome in advanced-stage SCC patients receiving curative chemoradiation with arterial cisplatin infusion has been demonstrated, although a few reports have described the utility of tumor blood flow or tumor micro-water diffusion as an evaluation tool during treatment using MRI (21,22). The results of the current study will provide supporting information for the prediction of treatment outcome; this information can be used for the adjustment of treatment regimens such as the addition of induction chemotherapy before curative therapy consisting of chemotherapy and concomitant full-dose radiotherapy, or the determination of a follow-up strategy after the treatment. In this way, the information gained from quantitative morphological parameters could lead to more appropriate personalized medicine in patients with nasal- or paranasal-cavity SCC.

The quantitative morphological characteristic of tumor sphericity is considered to reflect the tumor's complicated shape. In the case of an invasive tumor with a complicated shape, the feeding arteries tend to be multi-feeders compared to the simple expanding oval- or round-shape SCC, and this may make the arterial infusion therapy more complicated and difficult. FDG-PET/CT can easily visualize the rough shape of such anatomically complicated tumor by setting a specific SUV threshold. In contrast to

Table 3 ROC and multivariate analysis results

Parameter	The results of ROC curve analysis							The results of multivariate analysis	
	AUC	Sensitivity	Specificity	PPV	NPV	Accuracy	Cut-off value	P value	Odds ratio
Surface area	0.83	0.82	0.71	0.88	0.63	0.79	130	0.31	1.21 (0.87, 1.55)
Sphericity	0.87	0.82	1.0	1.0	0.7	0.88	0.31	0.03	2.58 (1.37, 6.74)

AUC, area under curve; PPV, positive predictive value; NPV, negative predictive value.

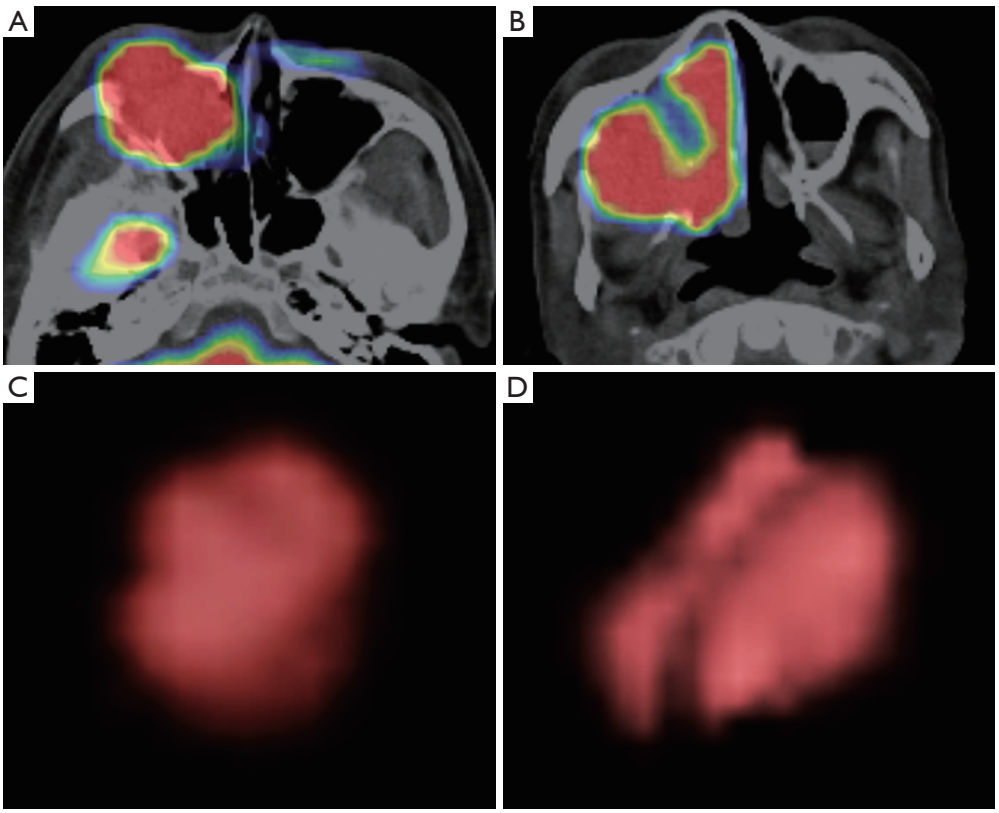

Figure 1 Representative cases of local control and failure. Pretreatment FDG-PET/CT fusion images from cases with local control (A) and failure (B) are shown. The volume rendering of FDG uptake in a lesion (SUV of upper 2.5, front view) from a patient with local control (C) had a less complicated shape compared to that of patient with treatment failure (D). The sphericities of the local control and failure cases were 0.43 and 0.29, respectively.

the parameter of sphericity, tumor volume was higher in the poor-treatment-outcome group, but not significantly so (P value =0.09). From the results of the current study, although tumor volume is generally believed to be a prognostic factor in numerous cancers, including head and neck SCC (23), quantitative information about tumor shape may be more sensitive for the prediction of treatment outcome. In addition, several previous reports have described that the tumor morphological parameter known as "asphericity" was useful as a prognostic factor in patients with HNSCC (24,25). Although their study population was somewhat heterogeneous (including primary sites of naso-, oro-, hypo-pharynx, lip and oral cavity) and did not include patients with nasal and paranasal cavity SCC, the parameter of quantitative tumor shape may be used for most HNSCC patients regardless of the primary site, by integrating the results of the current study and the previous reports described above.

Tumor heterogeneity was not found to be a prognostic factor in the current study. In several previous reports, the parameter of intratumoral heterogeneity was indicated to be a prognostic factor in advanced T-stage oropharyngeal SCC patients (10); higher intratumoral heterogeneity predicted a worse prognosis. The explanation of this discrepancy between studies is not straightforward. We speculated that the difference in treatment regimens—i.e., arterial infusion of cisplatin with concomitant radiotherapy versus systemic chemoradiation may have played a role, but we emphasize that this is only our supposition. In addition, the biological characteristics of oropharyngeal and maxillary cancer are slightly different (26) and may have led to the different results related to the intratumoral heterogeneity as a predictor of treatment outcome.

The current study has several limitations. First, the number of patients was very small. However, the patient population with nasal or paranasal SCC is generally rather

Table 4 Spearman's rank correlation coefficient to the sphericity

Variables	Correlation coefficient
T-stage	−0.32
N-stage	−0.19
SUVmean	−0.07
SUVmax	−0.2
CV	0.23
TLG	−0.17
Skewness	0.15
Kurtosis	0.07
Contrast	−0.11
Correlation	0.21
Energy	−0.24
Homogeneity	−0.28
Tumor volume	−0.21
Tumor surface area	−0.53
Sphericity	1

small. Second, analyses of correlations to other biological factors such as human papillomavirus (HPV) status or tumor histological grade were not performed. To address these limitations, further additional follow-up studies will be needed.

In conclusion, quantitative morphological evaluation of nasal or paranasal SCC by sphericity was indicated to be useful for the prediction of treatment outcome. This parameter could contribute to the appropriate tailoring of treatment strategy for patients with nasal or paranasal SCC.

Acknowledgements

None.

Footnote

Conflicts of Interest: The authors have no conflicts of interest to declare.

Ethical Statement: Our institutional review board approved this retrospective study protocol, and written informed consent was waived.

References

1. Wong SJ, Harari PM, Garden AS, Schwartz M, Bellm L, Chen A, Curran WJ, Murphy BA, Ang KK. Longitudinal Oncology Registry of Head and Neck Carcinoma (LORHAN): analysis of chemoradiation treatment approaches in the United States. Cancer 2011;117:1679-86.
2. Kimata Y, Uchiyama K, Ebihara S, Saikawa M, Hayashi R, Haneda T, Ohyma W, Kishimoto S, Asai M, Nakatsuka T, Harii K. Postoperative complications and functional results after total glossectomy with microvascular reconstruction. Plast Reconstr Surg 2000;106:1028-35.
3. Homma A, Oridate N, Suzuki F, Taki S, Asano T, Yoshida D, Onimaru R, Nishioka T, Shirato H, Fukuda S. Superselective high-dose cisplatin infusion with concomitant radiotherapy in patients with advanced cancer of the nasal cavity and paranasal sinuses: a single institution experience. Cancer 2009;115:4705-14.
4. Homma A, Sakashita T, Yoshida D, Onimaru R, Tsuchiya K, Suzuki F, Yasuda K, Hatakeyama H, Furusawa J, Mizumachi T, Kano S, Inamura N, Taki S, Shirato H, Fukuda S. Superselective intra-arterial cisplatin infusion and concomitant radiotherapy for maxillary sinus cancer. Br J Cancer 2013;109:2980-6.
5. Rohren EM, Turkington TG, Coleman RE. Clinical applications of PET in oncology. Radiology 2004;231:305-32.
6. Kitagawa Y, Sano K, Nishizawa S, Nakamura M, Ogasawara T, Sadato N, Yonekura Y. FDG-PET for prediction of tumour aggressiveness and response to intra-arterial chemotherapy and radiotherapy in head and neck cancer. Eur J Nucl Med Mol Imaging 2003;30:63-71.
7. Higgins KA, Hoang JK, Roach MC, Chino J, Yoo DS, Turkington TG, Brizel DM. Analysis of pretreatment FDG-PET SUV parameters in head-and-neck cancer: tumor SUVmean has superior prognostic value. Int J Radiat Oncol Biol Phys 2012;82:548-53.
8. Taghipour M, Sheikhbahaei S, Marashdeh W, Solnes L, Kiess A, Subramaniam RM. Use of 18F-Fludeoxyglucose-Positron Emission Tomography/Computed Tomography for Patient Management and Outcome in Oropharyngeal Squamous Cell Carcinoma: A Review. JAMA Otolaryngol Head Neck Surg 2016;142:79-85.
9. Moon SH, Choi JY, Lee HJ, Son YI, Baek CH, Ahn YC, Park K, Lee KH, Kim BT. Prognostic value of 18F-FDG PET/CT in patients with squamous cell carcinoma of the tonsil: comparisons of volume-based metabolic parameters. Head Neck 2013;35:15-22.

10. Cheng NM, Fang YH, Lee LY, Chang JT, Tsan DL, Ng SH, Wang HM, Liao CT, Yang LY, Hsu CH, Yen TC. Zone-size nonuniformity of 18F-FDG PET regional textural features predicts survival in patients with oropharyngeal cancer. Eur J Nucl Med Mol Imaging 2015;42:419-28.
11. Wang HM, Cheng NM, Lee LY, Fang YH, Chang JT, Tsan DL, Ng SH, Liao CT, Yang LY, Yen TC. Heterogeneity of (18)F-FDG PET combined with expression of EGFR may improve the prognostic stratification of advanced oropharyngeal carcinoma. Int J Cancer 2016;138:731-8.
12. Chan SC, Cheng NM, Hsieh CH, Ng SH, Lin CY, Yen TC, Hsu CL, Wan HM, Liao CT, Chang KP, Wang JJ. Multiparametric imaging using 18F-FDG PET/CT heterogeneity parameters and functional MRI techniques: prognostic significance in patients with primary advanced oropharyngeal or hypopharyngeal squamous cell carcinoma treated with chemoradiotherapy. Oncotarget 2017;8:62606-21.
13. Fujima N, Sakashita T, Homma A, Hirata K, Shiga T, Kudo K, Shirato H. Glucose Metabolism and Its Complicated Relationship with Tumor Growth and Perfusion in Head and Neck Squamous Cell Carcinoma. PLoS One 2016;11:e0166236.
14. Panin VY, Kehren F, Michel C, Casey M. Fully 3-D PET reconstruction with system matrix derived from point source measurements. IEEE Trans Med Imaging 2006;25:907-21.
15. Sato J, Kitagawa Y, Yamazaki Y, Hata H, Asaka T, Miyakoshi M, Okamoto S, Shiga T, Shindoh M, Kuge Y, Tamaki N. Advantage of FMISO-PET over FDG-PET for predicting histological response to preoperative chemotherapy in patients with oral squamous cell carcinoma. Eur J Nucl Med Mol Imaging 2014;41:2031-41.
16. Chang KP, Tsang NM, Liao CT, Hsu CL, Chung MJ, Lo CW, Chan SC, Ng SH, Wang HM, Yen TC. Prognostic significance of 18F-FDG PET parameters and plasma Epstein-Barr virus DNA load in patients with nasopharyngeal carcinoma. J Nucl Med 2012;53:21-8.
17. Lim R, Eaton A, Lee NY, Setton J, Ohri N, Rao S, Wong R, Fury M, Schöder H. 18F-FDG PET/CT metabolic tumor volume and total lesion glycolysis predict outcome in oropharyngeal squamous cell carcinoma. J Nucl Med 2012;53:1506-13.
18. Dhara AK, Mukhopadhyay S, Saha P, Garg M, Khandelwal N. Differential geometry-based techniques for characterization of boundary roughness of pulmonary nodules in CT images. Int J Comput Assist Radiol Surg 2016;11:337-49.
19. Nagano N, Matsuo T, Itoh T, Tomonari K, Shiraishi J. Development of a computer-aided diagnosis system for the distinction between benign and malignant gastric lesions. Nihon Hoshasen Gijutsu Gakkai zasshi 2012;68:1474-85.
20. Dang M, Lysack JT, Wu T, Matthews TW, Chandarana SP, Brockton NT, Bose P, Bansal G, Cheng H, Mitchell JR, Dort JC. MRI texture analysis predicts p53 status in head and neck squamous cell carcinoma. AJNR Am J Neuroradiol 2015;36:166-70.
21. Fujima N, Yoshida D, Sakashita T, Homma A, Tsukahara A, Tha KK, Kudo K, Shirato H. Usefulness of Pseudocontinuous Arterial Spin-Labeling for the Assessment of Patients with Head and Neck Squamous Cell Carcinoma by Measuring Tumor Blood Flow in the Pretreatment and Early Treatment Period. AJNR Am J Neuroradiol 2016;37:342-8.
22. Fujima N, Yoshida D, Sakashita T, Homma A, Tsukahara A, Shimizu Y, Tha KK, Kudo K, Shirato H. Prediction of the treatment outcome using intravoxel incoherent motion and diffusional kurtosis imaging in nasal or sinonasal squamous cell carcinoma patients. Eur Radiol 2017;27:956-65.
23. Strongin A, Yovino S, Taylor R, Wolf J, Cullen K, Zimrin A, Strome S, Regine W, Suntharalingam M. Primary tumor volume is an important predictor of clinical outcomes among patients with locally advanced squamous cell cancer of the head and neck treated with definitive chemoradiotherapy. Int J Radiat Oncol Biol Phys 2012;82:1823-30.
24. Apostolova I, Steffen IG, Wedel F, Lougovski A, Marnitz S, Derlin T, Amthauer H, Buchert R, Hofheinz F, Brenner W. Asphericity of pretherapeutic tumour FDG uptake provides independent prognostic value in head-and-neck cancer. Eur Radiol 2014;24:2077-87.
25. Hofheinz F, Lougovski A, Zöphel K, Hentschel M, Steffen IG, Apostolova I, Wedel F, Buchert R, Baumann M, Brenner W, Kotzerke J, van den Hoff J. Increased evidence for the prognostic value of primary tumor asphericity in pretherapeutic FDG PET for risk stratification in patients with head and neck cancer. Eur J Nucl Med Mol Imaging 2015;42:429-37.
26. Dok R, Nuyts S. HPV Positive Head and Neck Cancers: Molecular Pathogenesis and Evolving Treatment Strategies. Cancers (Basel) 2016;8(4).

Cite this article as: Fujima N, Hirata K, Shiga T, Yasuda K, Onimaru R, Tsuchiya K, Kano S, Mizumachi T, Homma A, Kudo K, Shirato H. Semi-quantitative analysis of pre-treatment morphological and intratumoral characteristics using ^{18}F-fluorodeoxyglucose positron-emission tomography as predictors of treatment outcome in nasal and paranasal squamous cell carcinoma. Quant Imaging Med Surg 2018;8(8):788-795. doi: 10.21037/qims.2018.09.09

